

## Enhancement of spontaneous emission in three-dimensional low refractive-index photonic crystals with designed defects

Zongsong Gan,<sup>1</sup> Baohua Jia,<sup>1</sup> Jing-Feng Liu,<sup>2,3</sup> Xue-Hua Wang,<sup>2,a)</sup> and Min Gu<sup>1,a)</sup>

<sup>1</sup>Centre for Micro-Photonics and CUDOS, Faculty of Engineering and Industrial Sciences, Swinburne University of Technology, Hawthorn, Victoria 3122, Australia

<sup>2</sup>State Key Laboratory of Optoelectronic Materials and Technologies, School of Physics & Engineering, Sun Yat-Sen University, Guangzhou 510275, China

<sup>3</sup>College of Science, South China Agriculture University, Guangzhou 510642, China

(Received 30 May 2012; accepted 31 July 2012; published online 14 August 2012)

In this work, we demonstrate that low refractive-index three-dimensional photonics crystals with a planar defect, fabricated with the direct laser writing method, can be used to effectively enhance the spontaneous emission (SE) of semiconductor quantum dots (QDs). To achieve this, we develop a controllable and reliable method to integrate quantum dots into the defect-embedded photonic crystals (PCs). Although the overlapping of different direction stop gaps in low refractive-index defect-free three-dimensional photonic crystals imposes a challenge to realize spontaneous emission enhancement at the band edge wavelength, we achieve a 15% enhancement of the spontaneous emission by introducing a tailored planar defect. © 2012 American Institute of Physics. [<http://dx.doi.org/10.1063/1.4745923>]

Defect is a key component for photonic crystal (PC) based applications such as photonic circuitry and waveguides,<sup>1</sup> resonant cavity,<sup>2</sup> and control of spontaneous emission (SE).<sup>3–5</sup> Although there have been a variety of experimental reports on the inhibition or enhancement of SE of internal emitters in colloidal PCs and polystyrene opals,<sup>6–9</sup> these structures are intrinsically challenging for controllable defect design, which prevents them from device applications. In comparison, the two-photon polymerization (2PP) based direct laser writing (DLW) method offers an unparalleled flexibility to fabricate high quality and sophisticated three-dimensional (3D) polymeric PCs with controllable defects.<sup>10–13</sup> More importantly, compared with other layer by layer semiconductor fabrication methods,<sup>14</sup> the 2PP method allows the easy incorporation of functional materials, such as quantum dots (QDs),<sup>15–17</sup> transforming the PCs into unique active platforms for diverse device applications. Inhibition of SE with PCs fabricated by the DLW method has been demonstrated previously.<sup>15–17</sup> However, due to the lack of controllable and reliable emitter integration method with the PCs, quantifying the enhancement of the SE correlated to the properties of the PCs represents a big challenge.

In this paper, we develop a controllable and reliable method to integrate semiconductor QDs into PCs. Based on this method, we quantitatively study the wavelength dependent property of SE enhancement with PCs fabricated by the 2PP method. The experimental results including a comparison with the SE inhibition match the theoretical predications well. Although the overlapping of different direction stop gaps prohibits the observation of the SE enhancement, the  $\Gamma$ -X direction stop gap band edge for PCs with refractive index as low as 1.526, introducing a designed planar defect in the middle of the PC, effectively modifies the photonic local

density of states (LDOS). As a result, a significant enhancement of the SE by more than 15% is realized.

As shown in Fig. 1(a) left, 3D woodpile PCs with 24 layers ( $60 \times 60 \mu\text{m}^2$  in size with a  $10 \mu\text{m}$  wide frame, a lattice constant of 1150 nm, and a refractive index  $n = 1.526$ , a typical refractive index value for PCs fabricated by the 2PP method.) were fabricated by the 2PP method with a photosensitive resin Ormocer (Micro Resist Technology) on a cover slip.<sup>18</sup> PbSe/CdSe core/shell (CS) QDs were synthesized according to references.<sup>19,20</sup> To ensure the QD fluorescence emitters are attached to the surface of the PC rods in a controllable way, a molecular linking method is used as shown in Figs. 1(b) and 1(c). For one layer of QD attachment, the polymerized Ormocer structures were first

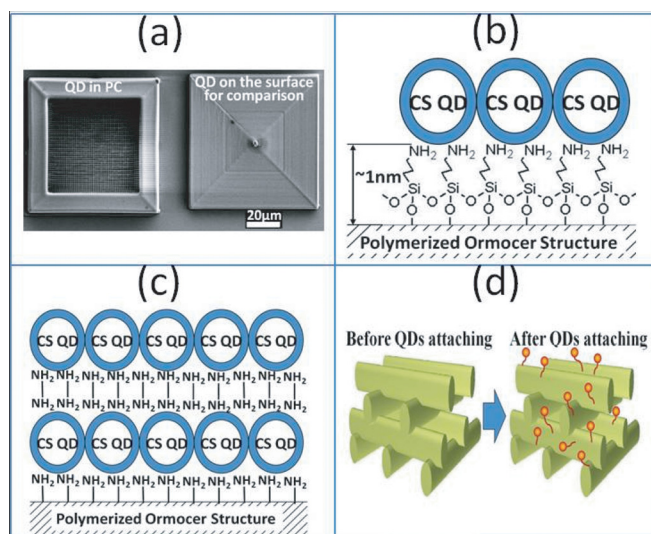


FIG. 1. Scanning electron microscope images of the 3D PC and the reference block. (b) Schematic illustration of one layer of QD attached to the polymer structure via the molecular linking method. (c) Schematic illustration of multi-layer QD attachment via the same method; (d) Schematic diagram of the fabricated PC and after the QD attachment.

<sup>a)</sup>Authors to whom correspondence should be addressed. Electronic addresses: wangxueh@mail.sysu.edu.cn and mgu@swin.edu.au.

functionalized with an amino group by immersing the structures into 3-aminopropyl-triethoxysilane (APTES) solution in toluene with 5% (v/v) concentration for 45 min. After washed with toluene, the structures were immersed into the highly concentrated PbSe/CdSe CS QD solution in toluene for 12 h to allow the QDs to connect to the functionalized structure surface via the molecular linking (Figs. 1(b) and 1(d)). For the multi-layer QD attachment, the above-mentioned process was repeated (Fig. 1(c)). To obtain enough fluorescence signals for the lifetime measurement, the QD attachment process was repeated 3 times and 4 layers of QDs are attached to the surface of the PC structure.

The transmission spectra of the PCs before and after the QD attachment were measured with a Fourier-transform infrared (FTIR) spectroscope. A stop gap can be clearly identified in the  $\Gamma$ -X direction as shown in Fig. 2. The emission spectrum of the attached QDs is also shown in Fig. 2 with the emission peak wavelength overlapping with the stop gap of the 3D PC. After 4 layers of QD attachment, the almost unchanged stop gap shape and the suppression ratio of the PC indicate that this QD attachment method is effective and does not induce clogging up of QDs, which would change the transmission spectrum significantly.

The fluorescence lifetime of the QDs was measured by a time-correlated single photon counting system in conjunction with a home-made confocal detection system with a high numerical aperture (NA = 0.8) objective.<sup>15,16</sup> The QDs were excited by a pulsed laser (1064 nm and 5 MHz). All the lifetime decay curves measured were fitted with a single exponential decay function as the excitation power was kept as low as possible to avoid the faster Auger recombination, and no significant exciton-exciton interaction was observed during the experiment due to the CdSe shelling of the QDs.<sup>21</sup>

The SE rate of the QDs is changed by the photonic LDOS in PCs compared with that in free space<sup>22</sup> and is characterized by the change of SE decay lifetime of the QDs. As the LDOS is position dependent and sensitive to the local environment,<sup>23,24</sup> in experiment, the design of the reference samples is of the same importance as the experimental samples. Different thicknesses of the QD layers and different materials that the QDs are in contact with can change the local refractive index and the non-radiative decay path of the QDs and lead to distorted results. An ideal situation is that the environments where the emitters in PCs and in the reference system are

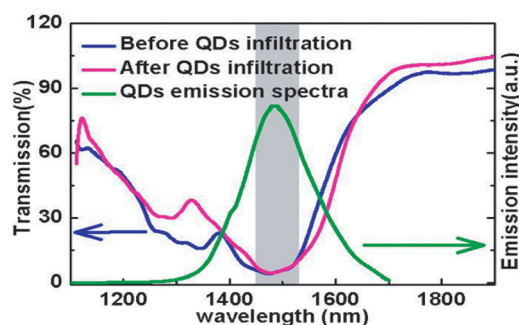


FIG. 2. Transmission spectrum of the PC in the  $\Gamma$ -X direction before and after the QD attachment and the emission spectra of the attached QDs with an emission peak wavelength matching the stop gap of the PC in the  $\Gamma$ -X direction. The shadow zone indicates the calculated wavelength range of the  $\Gamma$ -X direction stop gap.

identical except for the influence of the photonic LDOS of the PCs. In our experiment, this condition was realized by fabricating a square block near the side of the PC with the same material and the same fabrication power as the reference (Fig. 1(a) right). QDs were attached to the surface of this reference block via exactly the same molecular linking method. It was confirmed by the fluorescence intensity measurement that the QDs distributed statistically uniform inside the PCs and on the surface of the square block by using this controlled attachment method ensuring reliable comparison to be made.

Conventionally, the SE enhancement can be realized at the band edge.<sup>25</sup> To quantitatively investigate the band-edge related enhancement, the wavelength dependent property of controlling SE with the low refractive-index 3D PCs is studied. First, six PCs with the same parameters as the one shown in Fig. 1 with stop gaps in the  $\Gamma$ -X direction centered at wavelength of 1490 nm were fabricated. Then, six batches of PbSe/CdSe QDs with emission peaks at wavelengths of 1350 nm, 1400 nm, 1450 nm, 1480 nm, 1500 nm, and 1550 nm covering the stop gap as well as the band edges of the PCs were synthesized and attached to the surface of the rods of the PCs and the corresponding reference blocks.

For each of the sample and reference block, the SE lifetime were measured at the peak emission wavelength of the QDs for 60 different positions inside the PC and on the surface of the block to obtain the lifetime statistics. By comparing the average SE lifetime of QDs in the PCs and in the corresponding references, the impact of the stop gap on the SE of QDs can be determined. The wavelength dependent lifetime in the 3D PCs is shown in Fig. 3(a), in which the data have been normalized to the average lifetime of QDs on the reference. It is obvious that near the center of the stop gap (1490 nm), the highest SE inhibition of up to 20.5% was achieved.

It is interesting to note that even at the band edge of the  $\Gamma$ -X direction stop gap, the QD emission is still inhibited by more than 10%, which is no band-edge related emission enhancement for the PC with refractive index 1.526 was observed. This observation can be explained as follows: As shown in Fig. 3(b), in low refractive-index PCs, the stop gaps in different directions possess different gap wavelengths. This leads to the merge of the band edges with the adjacent stop gaps. In other words, the band edge enhancement behavior of a low refractive-index PC was blurred by the stop gaps in different directions. As a result, no enhancement can be realized in the PCs used in this work because the SE lifetime reflects the influence of stop gaps in all directions. This is different from high refractive-index PCs with complete band gaps, in which complete inhibition and significant enhancement can be achieved. The experimental results were confirmed by the theoretical calculations as shown in Fig. 3(a). The principle of the calculation is based on Refs. 23 and 24. The parameters used in the calculation were based on the experiment (woodpile PCs, refractive index: 1.526, lattice constant: 1150 nm; elliptical rod short axis: 175 nm, long axis: 350 nm; and 22 300 calculated positions in a basic unit). As shown in Fig. 3(a), the calculation fits the experiment well, showing exactly the same trend as the experiment.

It has been suggested that inducing defects such as a nano-cavity is an effective approach to enhance the emission as defects can change the LDOS in the PCs.<sup>5,26,27</sup> In our

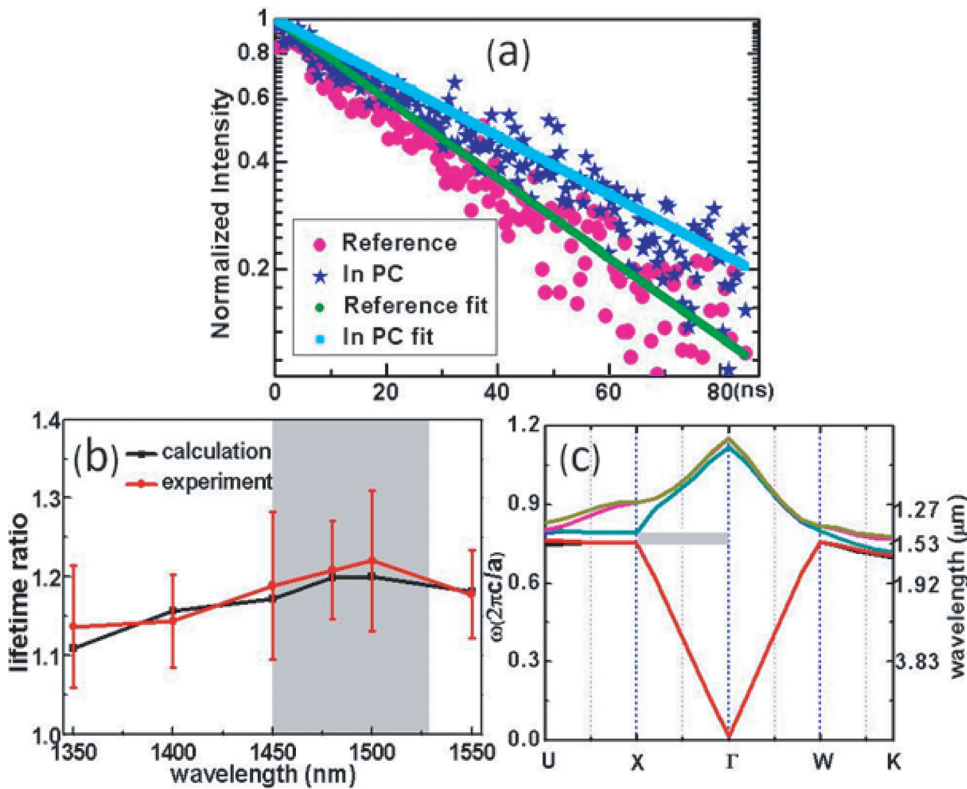


FIG. 3. (a) Typical decay curves fitted with single exponential decay function for QDs in PC and in the reference. (b) Experimental and calculation results of emission lifetime versus the wavelength for QDs inside the PCs compared with that in the reference; (c) Calculated photonic band diagram of the 3D stop gap PC with a refractive index 1.526. The shadow zone indicates the calculated wavelength range of the  $\Gamma$ -X direction stop gap.

experiment, planar defects were designed and fabricated by sandwiching an air gap (110% of the normal layer spacing) between two 12 layer ( $6\ \mu\text{m}$  in height) woodpile PCs. In Fig. 4(a), the FTIR spectrum confirms the successful inclusion of the planar defect, in which the defect mode centered at wavelength of 1450 nm exists within the wavelength range of the stop gap in the  $\Gamma$ -X direction. QDs with an emission peak matching the defect mode (1450 nm) of the PC with the planar defect were attached to the surfaces of the PCs and the reference block. SE lifetimes of QDs in the PCs with and without the planar defect were measured for different positions along the Z direction (perpendicular to the woodpile layer; the zero point plane in the Z direction was the up first layer). Due to the finite thickness of the fabricated PCs, it was expected that the maximum lifetime manipulation would be observed when the focal spot was placed in the middle of the PCs. For each Z position, 40 different positions were measured in one plane to obtain the lifetime statistics. Fig. 4(b) shows the Z direction lifetime response of QDs in the PCs with and without the planar defect compared with that in the reference block. For the PC without the planar

defect, a maximum prolonged lifetime was observed in the middle of the PC ( $Z = 6\ \mu\text{m}$ ) as expected. In comparison, for the PC with the planar defect, significant SE enhancement was observed when the focal spot was close to the defect ( $Z = 6\ \mu\text{m}$ ) as SE was determined by the LDOS of the local position where the emitter is.<sup>23,24</sup> A 35% decrease of QD emission lifetime was observed for the PC with the planar defect compared with that without the defect.

In conclusion, SE enhancement for QDs inside 3D low refractive-index defect-embedded PCs fabricated by the DLW method has been theoretically and experimentally studied. The comparative investigation based on the controllable method for the precise integration of quantum dots inside a PC has revealed not only the wavelength dependent SE inhibition up to 20.5% but also an SE enhancement up to 15% by inducing a planar defect. Our results suggest that low-index PCs can effectively control the SE, opening a possibility for them to be used directly for important photonic device applications, for example, the integrated micro lasers and micro-fluidic sensing.<sup>12</sup>

This research was conducted by the Australian Research Council Centre of Excellence for Ultrahigh Bandwidth Devices for Optical Systems (Project No. CE110001018). Baohua Jia is supported by the Australian Research Council Discovery Early Career Researcher Award DE120100291. Jing-Feng Liu and Xue-Hua Wang acknowledge the support from the National Basic Research Program of China (2010CB923200) and the National Natural Science Foundation of China (Grants 10725420 and U0934002).

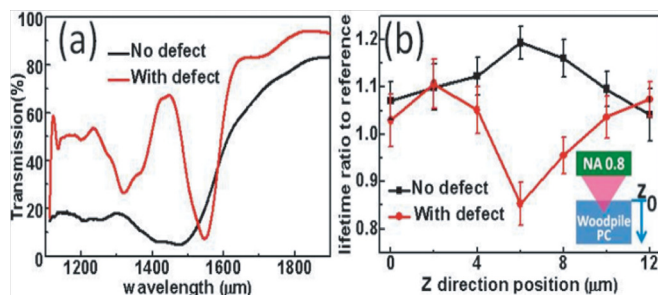


FIG. 4. (a)  $\Gamma$ -X direction transmission spectra of the PC with and without the plane defect; (b) Z direction lifetime response of QDs in the PC with and without the plane defect compared with the reference.

<sup>1</sup>M. Loncar, D. Nedeljkovic, T. Doll, J. Vuckovic, A. Scherer, and T. P. Pearsall, *Appl. Phys. Lett.* **77**, 1937 (2000).

<sup>2</sup>B. Temelkurana, E. Ozbay, J. P. Kavanaugh, G. Tuttle, and K. M. Ho, *Appl. Phys. Lett.* **72**, 2376 (1998).

<sup>3</sup>G. Liu, Y. Chen, and Z. Ye, *Sci. Technol. Adv. Mater.* **10**, 055001 (2009).

- <sup>4</sup>H. Y. Ryu and M. Notom, *Opt. Lett.* **28**, 2390 (2003).
- <sup>5</sup>W.-Y. Chen, W.-H. Chang, H.-S. Chang, T. M. Hsua, C.-C. Lee, C.-C. Chen, P. G. Luan, J.-Y. Chang, T.-P. Hsieh, and J.-I. Chyi, *Appl. Phys. Lett.* **87**, 071111 (2005).
- <sup>6</sup>F. D. Stasio L. Berti, M. Burger, F. Marabelli, S. Gardin, T. Dainese, R. Signorini, R. Bozio, and D. Comoretto, *Phys. Chem. Chem. Phys.* **11**, 11515 (2009).
- <sup>7</sup>M. Aleshyna, S. Sivakumar, M. Venkataramanan, A. G. Brolo, and F. C. J. M. van Veggel, *J. Phys. Chem. C* **111**, 4047 (2007).
- <sup>8</sup>M. R. Jorgensen, J. W. Galusha, and M. H. Bartl, *Phys. Rev. Lett.* **107**, 143902 (2011).
- <sup>9</sup>P. Lodahl, A. F. van Driel, I. S. Nikolaev, A. Irman, K. Overgaag, D. Vanmaekelbergh, and W. L. Vos, *Nature (London)* **430**, 654 (2004).
- <sup>10</sup>K. K. Seet, V. Mizeikis, S. Matsuo, S. Juodkazis, and H. Misawa, *Adv. Mater.* **17**, 541 (2005).
- <sup>11</sup>M. J. Ventura, M. Straub, and M. Gu, *Opt. Express* **13**, 2767 (2005).
- <sup>12</sup>J. Wu, D. Day, and M. Gu, *Appl. Phys. Lett.* **92**, 071108 (2008).
- <sup>13</sup>M. D. Leistikow, A. P. Mosk, E. Yeganegi, S. R. Huisman, A. Lagendijk, and W. L. Vos, *Phys. Rev. Lett.* **107**, 193903 (2011).
- <sup>14</sup>K. Aoki, D. Guimard, M. Nishioka, M. Nomura, S. Iwamoto, and Y. Arikawa, *Nat. Photonics* **2**, 688 (2008).
- <sup>15</sup>J. Li, B. Jia, G. Zhou, and M. Gu, *Opt. Express* **14**, 10740 (2006).
- <sup>16</sup>M. J. Ventura and M. Gu, *Adv. Mater.* **20**, 1329 (2008).
- <sup>17</sup>J. Li, B. Jia, G. Zhou, C. Bullen, J. Serbin, and M. Gu, *Adv. Mater.* **19**, 3276 (2007).
- <sup>18</sup>M. Gu, B. Jia, J. Li, and M. J. Ventura, *Laser Photon. Rev.* **4**, 414 (2010).
- <sup>19</sup>W. W. Yu, C. J. Falkner, S. B. Shih, and L. V. Colvin, *Chem. Mater.* **16**, 3318 (2004).
- <sup>20</sup>J. M. Pietryga, D. J. Werder, D. J. Williams, J. L. Casson, R. D. Schaller, V. I. Klimov, and J. A. Hollingsworth, *J. Am. Chem. Soc.* **130**, 4879 (2008).
- <sup>21</sup>M. Lee, J. Woon, S. Park, M. Kim, H. Seo, and J. J. Ju, *Nanotechnology* **16**, 1148 (2005).
- <sup>22</sup>Z. Li, L. Lin, and Z. Zhang, *Phys. Rev. Lett.* **84**, 4341 (2000); X. H. Wang, R. Wang, B. Y. Gu, and G. Z. Yang, *Phys. Rev. Lett.* **88**, 093902 (2002).
- <sup>23</sup>J.-F. Liu, H.-X. Jiang, C.-J. Jin, X.-H. Wang, Z.-S. Gan, B.-H. Jia, and M. Gu, *Phys. Rev. A* **85**, 015802 (2012).
- <sup>24</sup>J.-F. Liu, H.-X. Jiang, Z.-S. Gan, B.-H. Jia, C.-J. Jin, X.-H. Wang, and M. Gu, *Opt. Express* **19**, 11623 (2011).
- <sup>25</sup>K. Kuroda, Ts. Sawada, T. Kuroda, K. Watanabe, and K. Sakoda, *Opt. Express* **17**, 13168 (2009).
- <sup>26</sup>S. Ogawa, M. Imada, S. Yoshimoto, M. Okano, and S. Noda, *Science* **305**, 227 (2004).
- <sup>27</sup>J. Bao, M. Tabbal, T. Kim, S. Charnvanichborikarn, J. S. Williams, M. J. Aziz, and F. Capasso, *Opt. Express* **15**, 6727 (2007).